

Effect of 5-fluorouracil Carboxymethyl Chitosan Nanoparticles on the Apoptosis Level of Keloid Fibroblasts

Xiaoguang Su^{1*}, Bing Han², Xingdong Jia³, Yanjun Gao⁴

¹The Department of Plastic Surgery, The Second Hospital of Hebei Medical University, Shijiazhuang, 050000, China

²The Department of Thoraciccardio Surgery, PLA Rocket Force Characteristic Medical Center, Beijing, 100088, China

³The Department of General Surgery, Beijing Daxing District People's Hospital, Beijing, 102600, China

⁴The Department of Ophthalmology, The Second Hospital of Hebei Medical University, Shijiazhuang, 050000, China

Xiaoguang Su*: sxg76@163.com

Bing Han: jysyhan@126.com

Xingdong Jia: jxd3376@163.com

Yanjun Gao: gaoyanjunzzy@163.com

Abstract: Objective to investigate the effect of 5-fluorouracil (5-FU) loaded carboxymethyl chitosan (CMC) nanoparticles on the apoptosis level of keloid fibroblasts. Methods keloid tissue (n = 80) was taken from inpatient and outpatient patients who were treated in our hospital from January 2020 to December 2020. The fresh keloid specimen tissues were washed with saline three times. After removing the epithelium, they were cut into 2mm×2mm tissue blocks for subculture. CMC nanoparticles loaded with 5-FU were prepared by ionically crosslinking CMC solution with calcium chloride. The viability of fibroblasts was determined by MTT assay. Transwell was used to assess fibroblast invasion. The wound healing test was used to evaluate the migration of fibroblasts. The apoptotic cells were analyzed by Annexin V-FITC and flow cytometry. The expression of apoptotic protein in fibroblasts was determined by Western blot analysis. The expression of transforming growth factor-β (TGF-β) and Smad2/3 were analyzed by immunohistochemistry. The mRNA expression of ERK1/2, protein kinase B (AKT) and nuclear transcription factor-κB (NF-κB) was analyzed by RT-qPCR. Results compared with the control group, there was no difference in the viability of fibroblasts in the nanoparticle group at 0h ($P>0.05$), and the viability of fibroblasts at 24h, 48h and 72h decreased by 37.29%, 29.58% and 28.38, respectively ($P<0.05$). Compared with the control group, the fiber cells composed of nanoparticles were less likely to pass through the pores of the basement membrane and their invasiveness decreased ($P<0.05$). Compared with the control group, the migration ability of fibroblasts in the nanoparticle group decreased ($P<0.05$). Compared with the control group, the apoptotic

rate of fibers composed of nanoparticles increased ($P<0.05$). Compared with the control group, the expression levels of Bax, Caspase-3 and Caspase-9 apoptotic proteins in the nanoparticle group increased ($P<0.05$). Compared with the control group, the expression levels of TGF- β and Smad2/3 in the nanoparticle group decreased ($P<0.05$). Compared with the control group, the expression levels of ERK1/2, Akt and NF- κ B mRNA in the nanoparticle group decreased ($P<0.05$). Conclusion 5-FU loaded CMC nanoparticles could reduce fibrosis in keloids, lower cell proliferation, migration and invasion, and increase cell apoptosis by inhibiting TGF- β related pathways.

Keywords: 5-fluorouracil; Carboxymethyl chitosan; Nanoparticles; Keloids; Fibroblasts; Apoptosis

Tob Regul Sci.™ 2021;7(5): 2189-2198

DOI: doi.org/10.18001/TRS.7.5.134

1. Introduction

Due to the overgrowth of fibrous tissue in skin injury sites such as surgery, trauma, burn and body perforation, keloids are massive and tough [1]. Previous studies have reported that keloids are related to allergic and inflammatory reactions during wound healing [2]. However, the general mechanism of keloid formation has not been clarified. Every year, 11 million people worldwide suffer from keloids. In the past decades, various therapies have been proposed to treat keloids, including cryotherapy, surgery and intralesional injection of corticosteroids and chemotherapy drugs, such as bleomycin, mitomycin C and 5-FU [3-5]. In addition, various polymeric biomaterials have been used to care for chronic wounds and abnormal scars. One of them is CMC, which is a biodegradable chitosan derivative with unique biological activities, including antimicrobial activity, immune enhancement and wound healing [6]. In previous studies, CMC has been shown to inhibit the proliferation of keloid fibroblasts [7]. 5-FU is a pyrimidine analogue with antimetabolite activity [8]. One possible explanation for this activity is that 5-FU inhibits thymidine synthase, which is related to the conversion of uridine to thymidine. The synthesis of deoxyribonucleic acid is inhibited [9]. Therefore, 5-FU is commonly used to treat various cancers [10]. In this study, CMC was used as a carrier to provide 5-FU. CMC nanoparticles loaded with 5-FU were prepared by gelation method. The influence of CMC

nanoparticles loaded with 5-FU on the keloid fibroblasts apoptosis level was explored.

2. Materials and Methods

2.1. Clinical sample collection

All specimens were taken from inpatients and outpatients who were treated in our hospital from January 2020 to December 2020. Keloid tissue (n=80) was taken from patients diagnosed by pathological diagnosis. Patients suffering from cancer and genetic/infectious diseases were excluded from this project. The participants had received radiotherapy and chemotherapy before surgery. In addition, the informed consent of the participants was obtained, and the research was approved by the hospital and its ethics committee.

2.2. Isolation and culture of fibroblasts

The cut fresh keloid tissue was washed with saline for 3 times, and cut into 2mm×2mm tissue blocks after epithelial removal. After spreading on sterile culture bottle, fibroblasts were cultured in 5%CO₂ at 37°C for 4 hours. The culture medium was changed every 3 to 4 days, and the fibroblasts were digested in 0.25% trypsin. The fibroblasts grew and covered the bottom for passage culture. After three passages, fibroblasts were cultured in Dulbecco modified Eagle medium (DMEM) containing 10% fetal bovine serum (FBS) at 37°C in 5%CO₂.

2.3. Preparation of CMC nanoparticles loaded with 5-Fu

CMC nanoparticles loaded with 5-FU were prepared by ionic crosslinking CMC solution with calcium chloride. 0.05% (w/v) CMC with 0.1%

(v/v) Tween 80 was dissolved in distilled water. Each type of 0.5% (w/v) CMC and 5-FU (2 mg/ml) solution was prepared. The 5-FU solution was added to the CMC solution at a volume ratio of 1: 9 and stirred overnight. For CMC nanoparticles without drugs, distilled water of the same volume was added to replace 5-FU. CaCl₂ solution was added to CMC solution with 5-FU under magnetic stirring to obtain CMC nanoparticles loaded with 5-FU. With the formation of particles, transparent solution spontaneously became milky white emulsion by Tindal effect. Particles were separated by centrifugation at 10,000 rpm at 4°C for 5 minutes. The precipitate was dispersed in distilled water and lyophilized. The obtained nanoparticles were stored at 4°C for further study.

2.4. Determination of the activity of fibroblasts by MTT assay

Accurate 1×10^4 fibroblasts were mixed with 100µL culture solution and inoculated into each well of 96-well culture plate. The fibroblasts were cultured for 12, 24, 48 and 72 hours, respectively, and then 20µL MTT solution (Genechem, China) with a concentration of 5g/L was added to each well. 150µL dimethyl sulfoxide was added to each well to dissolve the blue-violet crystal. After gently shaking the solution in the dark for 10 minutes, the optical density (OD [490]) of each well was measured with a microplate reader at a wavelength of 490 nm.

2.5. Cell invasion determination

Transwell coated with Matrigel (BD Biosciences, USA) was used to evaluate the invasion of fibroblasts. About 2×10^4 cells in 200µL serum-free DMEM medium were inoculated into the upper chamber, and the lower chamber was filled with Dulbecco modified Eagle medium (DMEM, Gibco, USA) and 10%FBS, with a total volume of 500µL. After 24 hours of culture, invasive cells that passed through the Matrigel barrier on the bottom surface of the membrane were fixed with methanol and stained with crystal violet. The image was taken with an inverted microscope. The determination was made in quadruplicate and repeated with 3 cell samples.

2.6. Determination of cell migration

Cells were uniformly (2×10^5 cells/well) inoculated into a six-well plate and cultured for 24 hours. The plate was kept overnight at 37°C and in 5% CO₂ in a humid atmosphere to obtain the fused cell monolayer. The cell wound was scrapped with a sterile 200µL pipette tip. The non-adhered cells with PBS were washed off. The cells were cultured and incubated with fresh medium without supplement for 24 hours. The cell migration was observed, and pictures of each hole were taken with an objective inverted microscope (Olympus, Japan). The result was expressed as a percentage of scratch area filled with cells. Data were obtained from four randomly selected high power fields. The determination was made in quadruplicate and repeated with 3 cell samples.

2.7. Apoptosis analysis by flow cytometry

Transfected cells were placed in a 6-well plate at a density of 2×10^5 cells/well, and centrifuged at $5,000 \times g$ for 5 minutes at room temperature. Cell pellet was washed with PBS and resuspended in wells. Cells were incubated with 5µl propidium iodide (Thermo Fisher Scientific) in the dark at 4°C for 30 minutes, and stained with 5µl Annexin V-FITC for 15 minutes at room temperature (catalog number ab1408; Abcam). Then, flow cytometry (BD Biosciences) and FlowJo software (version 7.6; FlowJo LLC) were used to analyze the apoptotic cells.

2.8. Western blot analysis

After adding RIPA buffer (Pierce), fibroblasts were lysed for 30 minutes, and the obtained cleavage products were centrifuged at 12000g for 10 minutes. The supernatant was collected and the total protein concentration was measured according to the strength of BCA kit (Pierce). Then, 50µg protein was extracted from each sample, and 12% sodium dodecyl sulfate-polyacrylamide gel electrophoresis was carried out on the spacer gel at 80 V for 40 minutes and on the separation gel at 120 V for 1.5 hour. The protein was transferred to PVDF membrane at 100 V and sealed in 5% skim milk powder at room

temperature for 1 hour. After that, the proteins were incubated at 4°C overnight for Bax (1: 5000), Caspase-3 (1:500), Caspase-9 (1: 1000), and glyceraldehyde-3-phosphate dehydrogenase (GAPDH). The next day, after supplementing horseradish peroxidase labeled goat anti-rabbit secondary antibody, the protein was incubated at 37°C for another 2 hours. ScionImage software was used to measure the gray value of protein band with GAPDH as internal reference.

2.9. Histological and immunohistochemical evaluation

The keloids and normal tissues were fixed in 10% formalin buffer, treated with nanoparticles, embedded in paraffin blocks, and sliced with a thickness of 5µm. The slices were stained with hematoxylin and eosin (H&E). Immunohistochemistry (IHC) was performed in keloid tissue and keloid spheroid. Tissues were incubated with the following primary antibodies, including TGF-β and SMAD2/3 (Cell Signaling Technology, Danvers, Massachusetts, USA). After washing with phosphate buffer (PBS), the slides were incubated with secondary antibody (Santa Cruz Biotechnology, Santa Cruz, California, USA). All slides were stained with hematoxylin. Semi-quantitative analysis of factor expression level was carried out by computer-aided planar method (Universal Image, Buckinghamshire, UK). The result was expressed as the average optical density of six different digital images.

2.10. RT-qPCR

According to the manufacturer's procedures, reagents (Invitrogen) was used to extract RNA from tissues/cells, and the NanoDrop 1000 spectrophotometer (Thermo Fisher Scientific, Inc.) was used to determine the concentration. The quality of the extracted RNA was evaluated using an Agilent 2100 bioanalyzer (Agilent Technologies GmbH), and the ratio of 28S: 18S was > 1.0. PrimeScript™RT kits (Takara Biotechnology Co, ltd.) were used to synthesize cDNA. Samples were incubated at room temperature for 30 minutes, at 42°C for 45

minutes, at 99°C for 5 minutes, and at 5°C for 5 minutes in the PCR cycler. Then, qPCR was performed using SYBR Green PCR Master Mix (Takara Biotechnology Co., Ltd.) according to the manufacturer's procedures. The qPCR adopted the following thermal cycling conditions: initial denaturation at 95°C for 5 minutes, denaturation at 95°C for 45 cycles for 15 seconds, annealing at 60°C for 20 seconds, extension at 72°C for 10 seconds, and finally extension at 72°C for 10 minutes. The relative expression level was calculated by $2^{-\Delta\Delta C_t}$ method (13), and normalization was carried out with respect to the internal reference gene GAPDH.

2.11. Statistical analysis

SPSS 21.0 software (SPSS Inc, Chicago, IL) or Graphpad Prism 6 software were used to analyze all experimental data. The measurement data displayed as mean±standard deviation (SD) were compared by Student t-test and one-way ANOVA. $P<0.05$ indicated statistically significant comparison.

3. Results

3.1. Inhibition of the activity of fibroblasts by nanoparticles

Compared with the control group, the activity of fibroblasts in the nanoparticle group had no difference at 0h ($P>0.05$), but decreased by 37.29%, 29.58% and 28.38 ($P<0.05$) at 24h, 48h and 72h respectively as shown in Figure 1, Table 1.

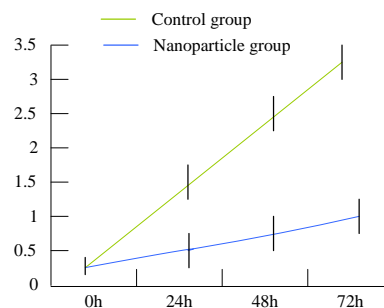


Figure 1. The activity of fibroblasts

Table 1. The activity of fibroblasts

Group	0h	24h	48h	72h
Control group	0.3	1.5	2.5	3.3
Nanoparticle group	0.3	0.5	0.8	1.0

Control group	0.13±0.06	1.18±0.17	2.13±0.22	2.96±0.15
Nanoparticle group	0.11±0.03	0.44±0.13	0.63±0.12	0.84±0.11
<i>t</i> value	7.927	5.728	9.738	8.726
<i>p</i> value	0.414	0.013	0.007	<0.001

3.2. Inhibition of the invasion and migration of fibroblasts by nanoparticles

Transwell analysis showed that, compared with the control group, the fibroblast cells of the nanoparticle group were less likely to pass through basement membrane, with lower invasiveness ($P < 0.05$). On the other hand, the results of wound healing test showed that the migration ability of fibroblasts in the nanoparticle group was lower than in the control group ($P < 0.05$) as shown in Figure 2, Table 2.

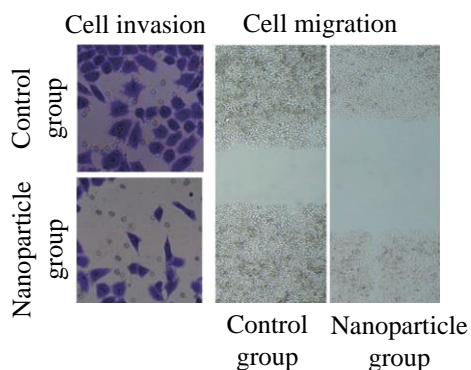


Figure 2. Invasion and migration of fibroblasts

Table 2. Invasion and migration of fibroblasts

Group	Cell invasion	Cell migration (%)
Control group	115.44±13.72	62.82±4.82
Nanoparticle group	54.78±8.92	28.44±3.12
<i>t</i> value	8.829	7.929
<i>p</i> value	0.012	0.004

3.3. Promotion of fibroblast apoptosis by nanoparticles

The apoptosis rate of fibroblasts was analyzed by

flow cytometry. Compared with the control group, the apoptosis rate of fibroblasts in the nanoparticle group increased ($P < 0.05$) as shown in Figure 3, Table 3.

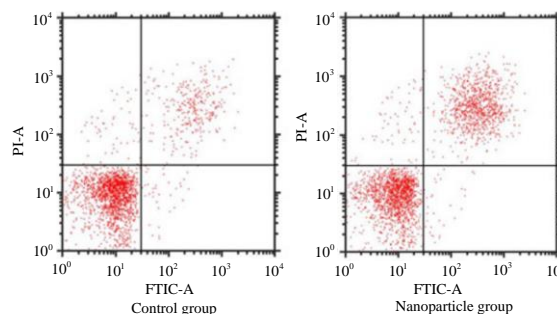


Figure 3. Apoptosis analysis by flow cytometry

Table 3. Apoptosis rate of fibroblasts

Group	Apoptosis rate (%)
Control group	4.33±0.32
Nanoparticle group	18.47±1.79
<i>t</i> value	7.827
<i>P</i> value	0.007

3.4. Promotion of expression of apoptosis proteins by nanoparticles

Compared with the control group, the expression levels of Bax, Caspase-3 and Caspase-9 apoptosis proteins in nanoparticle group increased ($P < 0.05$) as shown in Table 4.

Table 4. Expression of Bax, Caspase-3 and Caspase-9 apoptosis proteins

Group	Bax	Caspase-3	Caspase-9
Control group	1.33±0.26	1.77±0.13	1.36±0.12
Nanoparticle group	5.47±0.33	7.72±0.15	6.33±0.14
<i>t</i> value	7.927	6.728	7.827
<i>P</i> value	0.012	0.013	0.012

3.5. Inhibition of expression of TGF-β and Smad2/3 by nanoparticles

Immunohistochemical analysis of TGF-β and Smad2/3 showed that TGF-β and Smad2/3 expression levels in the nanoparticle group were

lower than those in the control group ($P < 0.05$) as shown in Table 5.

Table 5. Average optical density ($\times 10^4$)

Group	TGF- β	Smad2 / 3
Control group	13.88 \pm 1.27	15.76 \pm 1.88
Nanoparticle group	2.25 \pm 0.34	2.15 \pm 0.34
<i>t</i> value	3.729	7.917
<i>P</i> value	<0.001	<0.001

3.6. Inhibition of expression of ERK1/2, Akt and NF- κ B mRNA by nanoparticles

The mRNA expression of ERK1/2, Akt and NF- κ B was analyzed by RT-qPCR. Compared with the control group, the mRNA expression levels of ERK1/2, Akt and NF- κ B in the nanoparticle group decreased ($P < 0.05$) as shown in Table 6.

Table 6. Expression of ERK1/2, Akt and NF- κ B mRNA

Group	ERK1/2	Akt	NF- κ B
Control group	2.33 \pm 0.1 2	1.89 \pm 0.1 4	2.22 \pm 0.1 5
Nanoparticle group	1.05 \pm 0.1 3	1.03 \pm 0.1 1	1.04 \pm 0.1 2
<i>t</i> value	5.172	7.817	5.816
<i>P</i> value	0.023	0.027	0.014

4. Discussion

Keloid is an abnormal scar caused by skin injury (such as trauma, burn and surgery). Regarded as a benign fibroproliferative tumor, it eventually leads to abnormal skin fibrosis, and is characterized by excessive deposition of extracellular matrix [11]. Usually, these tumors invade adjacent normal tissues, and rarely spontaneously subside. Compared with the in/out-of-focus area, the collagen I and III produced by fibroblasts growing at the edge of keloid will increase [12]. Keloid is too large in the initial injury area and is characterized by itching and pain. According to previous studies, some gene regulators, including cytokines and chemokines, participate in the formation and development of keloids [13]. In recent years, people are increasingly interested in pathological scars.

Although there is no clear understanding of the potential mechanism of keloids, it has been found that several mediating factors can affect the pathogenesis of keloids. Excessive extracellular matrix caused by uncontrolled proliferation of keloid fibroblasts is one of the most famous causes of keloid formation. Therefore, it is generally considered that keloid formation is caused by the increase of cell proliferation and the decrease of apoptosis rate in keloid fibroblasts [14]. Appropriate treatment may be aimed at inhibiting the proliferation of keloid fibroblasts or reversing pathological fibrosis.

Previous studies have shown that CMC effectively prevents the growth of keloid fibroblasts [15]. In addition, 5-FU is a promising method with antimetabolite activity to treat abnormal scars. For local delivery of CMC nanoparticles loaded with 5-FU, we used coated microneedles. The manufactured stainless steel microneedle array was coated with the preparation including nanoparticles. The formula was optimized to improve the loading efficiency of particles. The coating preparation is composed of tackifier, surfactant, particle stabilizer and nanoparticle group. CMC is used to enhance the viscosity of the formula. Lutrol-F68 can improve the loading efficiency of particles by reducing the surface tension of microneedles. Trehalose enhances the stability of granules. Pilot-scale experiment was carried out to find the best proportion and concentration of coating solution. The preparation is composed of 1% (w/v) CMC, 0.5% (w/v) Lutrol F68, 15% (w/v) trehalose and 2% 5-FU loaded CMC nanoparticles. The composition of the coating formula makes the nanoparticles stable and has the best viscosity for dip coating process. The size of nanoparticles in the preparation by DLS was evaluated. As a result, it was confirmed that the nanoparticles were stable in the coating formulation because the size of the nanoparticles did not change significantly. The microneedle array was precoated with 2% (w/v) CMC solution to minimize the influence of humidity. As the test result of optimizing the

optimum thickness, the coating was repeated 12 times. We observed that CMC nanoparticles loaded with 5-FU inhibited the proliferation, migration and invasion of keloid fibroblasts and promoted the apoptosis of keloid fibroblasts.

Various cytokines, including TGF- β , vascular endothelial growth factor, platelet-derived growth factor, interleukin-1, interleukin-6, tumor necrosis factor- α and insulin-like growth factor-1, are considered to promote the formation of keloid [16-18]. Activation of the AKT and NF- κ B pathways is associated with mediating invasiveness. TGF- β , AKT and NF- κ B pathway affect some parts of wound healing process, such as cell migration, proliferation and extracellular matrix maturation, and keloid formation [19]. TGF- β signal transduction has become the core pathway of fibroblast activation. TGF- β is the key factor of keloid hyperplasia and collagen synthesis, because it enhances mitotic response [20]. TGF- β 1 increases the synthesis of collagen and fibronectin in fibroblasts. Overexpression of TGF- β 1 in keloid fibroblasts has been observed. This abnormal expression leads to keloid formation, which is the result of increased production of collagen and matrix metalloproteinase. Smad2/3, ERK1/2 complex, Akt and NF- κ B, the key mediators of TGF- β signaling pathway, are highly activated in keloids, which is related to the pathogenesis of keloids. 5-FU is a fluorinated pyrimidine analogue with antimetabolism activity. The mechanism of its activity is not clear, but many experiments show that 5-FU inhibits the proliferation of keloid fibroblasts by inhibiting the expression of TGF- β 1. We found that 5-FU loaded CMC nanoparticles decreased the expression of TGF- β , Smad2/3, ERK1/2 complex, Akt and NF- κ B in keloid spheres. In a word, these results indicate that CMC nanoparticles loaded with 5-FU has an effective anti-fibrosis effect on keloids. To sum up, 5-FU loaded CMC nanoparticles could reduce fibrosis in keloids, decrease cell proliferation, migration and invasion, and increase cell apoptosis by inhibiting TGF- β related pathways.

These results indicate that 5-FU loaded CMC nanoparticles is a new strategy to treat keloids [21-27].

References

1. Wang X.M., Liu X.M., Wang Y., et al., Activating transcription factor 3 (ATF3) regulates cell growth, apoptosis, invasion and collagen synthesis in keloid fibroblast through transforming growth factor beta (TGF-beta)/SMAD signaling pathway, *Bioengineered*, 2021, 12, 117-126.
2. Han B., Fan J., Liu L., et al., Adipose-derived mesenchymal stem cells treatments for fibroblasts of fibrotic scar via downregulating TGF- β 1 and Notch-1 expression enhanced by photobiomodulation therapy, *Lasers Med Sci*, 2019, 34, 1-10.
3. Tu T., Huang J., Lin M., et al., CUDC-907 reverses pathological phenotype of keloid fibroblasts in vitro and in vivo via dual inhibition of PI3K/Akt/mTOR signaling and HDAC2, *Int J Mol Med*, 2019, 44, 1789-1800.
4. Lv W., Liu S., Zhang Q., et al., Downregulation of epac reduces fibrosis and induces apoptosis through akt signaling in human keloid fibroblasts, *J Surg Res*, 2021, 257, 306-316.
5. Yang D., Li M., Du N., Effects of the circ_101238/miR-138-5p/CDK6 axis on proliferation and apoptosis keloid fibroblasts, *Exp Ther Med*, 2020, 20, 1995-2002.
6. Liu T., Ma X., Ouyang T., et al., Efficacy of 5-aminolevulinic acid-based photodynamic therapy against keloid compromised by downregulation of SIRT1-SIRT3-SOD2-mROS dependent autophagy pathway, *Redox Biol*, 2019, 20, 195-203.
7. Zhang L., Qin H., Wu Z., et al., Gene expression profiling analysis: the effect of hydrocortisone on keloid fibroblasts by bioinformatics, *J Dermatolog Treat*, 2019, 30, 200-205.
8. Cui X., Zhu J., Wu X., et al., Hematoporphyrin monomethyl ether-mediated photodynamic therapy inhibits the growth of keloid graft by promoting fibroblast apoptosis and reducing vessel formation, *Photochem Photobiol Sci*, 2020, 19, 114-125.
9. Lei R., Li J., Liu F., et al., HIF-1 α promotes the keloid development through the activation of TGF- β /Smad and TLR4/MyD88/NF- κ B pathways, *Cell Cycle*, 2019, 18, 3239-3250.
10. Wang M., Chen L., Huang W., et al., Improving the anti-keloid outcomes through liposomes loading paclitaxel-cholesterol complexes, *Int J Nanomedicine*, 2019, 14, 1385-1400.
11. Li X., Chen Z., Li X., et al., In vitro analysis of the role of tumor necrosis factor-stimulated gene-6 in keloid, *Mol Med Rep*, 2019, 19, 919-926.

12. Yan L., Wang L.Z., Xiao R., et al., Inhibition of microRNA-21-5p reduces keloid fibroblast autophagy and migration by targeting PTEN after electron beam irradiation, *Lab Invest*, 2020, 100, 387-399.
13. Zhou Y., Sun Y., Hou W., et al., The JAK2/STAT3 pathway inhibitor, AG490, suppresses the abnormal behavior of keloid fibroblasts in vitro, *Int J Mol Med*, 2020, 46, 191-200.
14. Cui J., Li Z., Jin C., et al., Knockdown of fibronectin extra domain B suppresses TGF- β 1-mediated cell proliferation and collagen deposition in keloid fibroblasts via AKT/ERK signaling pathway, *Biochem Biophys Res Commun*, 2020, 526, 1131-1137.
15. Wang Z., Feng C., Song K., et al., lncRNA-H19/miR-29a axis affected the viability and apoptosis of keloid fibroblasts through acting upon COL1A1 signaling, *J Cell Biochem*, 2020, 121, 4364-4376.
16. Jin J., Jia Z.H., Luo X.H., et al., Long non-coding RNA HOXA11-AS accelerates the progression of keloid formation via miR-124-3p/TGF β R1 axis, *Cell Cycle*, 2020, 19, 218-232.
17. Pang Q., Wang Y., Xu M., et al., MicroRNA-152-5p inhibits proliferation and migration and promotes apoptosis by regulating expression of Smad3 in human keloid fibroblasts, *BMB Rep*, 2019, 52, 202-207.
18. Wu J., Fang L., Cen Y., et al., MiR-21 Regulates Keloid Formation by Downregulating Smad7 via the TGF- β /Smad Signaling Pathway, *J Burn Care Res*, 2019, 40, 809-817.
19. Si L., Zhang M., Guan E., et al., Resveratrol inhibits proliferation and promotes apoptosis of keloid fibroblasts by targeting HIF-1 α , *J Plast Surg Hand Surg*, 2020, 54, 290-296.
20. Jian X., Qu L., Wang Y., et al., Trichostatin A-induced miR-30a-5p regulates apoptosis and proliferation of keloid fibroblasts via targeting BCL2, *Mol Med Rep*, 2019, 19, 5251-5262.
21. Darvishi, E., Kahrizi, D., Arkan, E., Hosseinabadi, S. and Nematpour, N., 2021. Preparation of bio-nano bandage from quince seed mucilage/ZnO nanoparticles and its application for the treatment of burn. *Journal of Molecular Liquids*. 339:116598.
22. Khaledian, S., Noroozi-Aghideh, A., Kahrizi, D., Moradi, S., Abdoli, M., Ghasemalian, A.H., and Heidari, M.F. 2021. Rapid detection of diazinon as an organophosphorus poison in real samples using fluorescence carbon dots. *Inorganic Chemistry Communications*. 130:108676.
23. Khaledian, S., Kahrizi, D., Moradi, S. and Martinez, F., 2021. An experimental and computational study to evaluation of chitosan/gum tragacanth coated-natural lipid-based nanocarriers for sunitinib delivery. *Journal of Molecular Liquids*. 334:116075.
24. Khaledian, S., Kahrizi, D., Balaky, S.T., Arkan, E., Abdoli, M. and Martinez, F. 2021. Electrospun nanofiber patch based on gum tragacanth/polyvinyl alcohol/molybdenum disulfide composite for tetracycline delivery and their inhibitory effect on Gram⁺ and Gram⁻ bacteria. *Journal of Molecular Liquids*. 334:115989.
25. Olfati, A., Kahrizi, D., Balaky, S.T., Sharifi, R., Tahir, M.B. and Darvishi, E. 2021. Green synthesis of nanoparticles using *Calendula officinalis* extract from silver sulfate and their antibacterial effects on *Pectobacterium caratovorum*. *Inorganic Chemistry Communications*. 125:108439.
26. Mirmoeini, T., Pishkar, L., Kahrizi, D., Barzin, G. and Karimi, N. 2021. Phytotoxicity of green synthesized silver nanoparticles on *Camelina sativa* L. *Physiology and Molecular Biology of Plants*. 27(2):pp 417-27.
27. Rahimi, T., Kahrizi, D., Feyzi, M., Ahmadvandi, H.R. and Mostafaei, M. 2021. Catalytic performance of MgO/Fe₂O₃-SiO₂ core-shell magnetic nanocatalyst for biodiesel production of *Camelina sativa* seed oil: Optimization by RSM-CCD method. *Industrial Crops and Products*. 159: 113065.

[1]



Xiaoguang Su, 1976.7, Male, Deputy Chief Physician, From 1995 to 2000, he graduated from clinical medicine of Hebei Medical University with bachelor degree; From 2009 to 2012, he graduated from Hebei Medical University, majoring in surgery, master's degree, Now working in the second hospital of Hebei Medical University, The direction of academic research is surface plastic surgery and cosmetic surgery, He has published more than 15 academic articles and obtained three scientific and technological achievements in Hebei Province.



Bing Han, 1976.6, Male, Deputy Chief Physician, From 1995 to 2000, he graduated from clinical medicine of Hebei Medical University with bachelor degree; From 2000 to 2003, he graduated from Hebei Medical University, majoring in surgery, master's degree, Now working in Director of thoracic surgery, rocket army characteristic medical center, The direction of academic research is minimally invasive surgery for lung cancer, He has published 25 articles, participated in one national 863 project and won two third prizes of military medical achievements.



Xingdong Jia, 1976.11, Male, Deputy Chief Physician, From 1995 to 2000, he graduated from clinical

Xiaoguang Su et al.

Effect of 5-fluorouracil Carboxymethyl Chitosan Nanoparticles on the Apoptosis Level of Keloid Fibroblasts

medicine of Hebei Medical University with bachelor degree, Now working in Beijing Daxing District People's Hospital, The direction of academic research is thyroid and breast surgery, He has 1 article published.



Yanjun Gao, 1977.1, Male, Deputy Chief Physician, From 1995 to 2000, he graduated from clinical medicine of Hebei Medical University with bachelor degree, From 2000 to 2003, graduated from ophthalmology of Hebei Medical University, master's degree, In 2011, he studied in the second hospital of Hebei Medical University, majoring in surgery (Ophthalmology), He is studying for a doctor's degree, Now working in Department of Ophthalmology, the second hospital of Hebei Medical University, The direction of academic research is orbital disease, ocular trauma, eye tumor, etc, He has published more than 10 articles and obtained three scientific and technological achievements in Hebei Province.